

Self-diffusion near the percolation threshold in reverse microemulsions

Brian Antalek, Antony J. Williams, and John Texter

Analytical Technology Division, Eastman Kodak Company, Rochester, New York 14650

(Received 7 May 1996)

Self-diffusion measurements of reverse water–acrylamide–sodium bis(2-ethylhexyl)sulfosuccinate–toluene microemulsions have identified a distinct increase in water proton diffusion above the percolation threshold in cosurfactant chemical potential. This increase is assigned to water transport through fractal aggregates and clusters. Above threshold, increasing apparent partitioning of water and cosurfactant into the continuous pseudophase yields an order parameter for estimating percolating cluster volume, and shows that cosurfactant preferentially segregates into these clusters. [S1063-651X(96)50612-4]

PACS number(s): 82.70.Kj, 05.70.-a, 05.60.+w, 47.20.Ma

Reverse microemulsions of water suspended as nanodroplets in a continuous pseudophase of water immiscible solvent, where these nanodroplets are stabilized by a monolayer of surfactant, are of continuing physical and chemical interest [1]. A particularly important transport property of interest in these systems is electrical conductivity, and the increase of conductivity above percolation thresholds in temperature, volume fraction, or other field variable.

One of the key structural features associated with reverse microemulsions, besides the details of the droplet composition, diameter, and the interfacial arrangement of surfactant between the water and oil, is the interaction of such particles in forming clusters and aggregates, and the relation of such aggregation to percolation. In addition, a fascinating and yet unresolved issue is the mechanism of transformation of reverse microemulsions into bicontinuous microemulsions having low to zero mean curvature (so-called sponge phase or middle phase microemulsions). Controversy persists [2–4] in experimentally distinguishing reverse and bicontinuous microemulsions, and whether percolation itself indicates a transformation to sponge phase bicontinuity [5–7] or the formation of particle clusters [8,9]. Chen, Chang, and Strey [10] have mapped out a cohesive picture that leads from reverse microemulsion droplets to droplet clusters and aggregates to bicontinuous connectivity. Percolation in reverse microemulsions has been described as arising from increased transport from particle aggregation and clustering [11,12]. On the other hand, percolation is sometimes taken as *de facto* proof of sponge phase bicontinuity. The differences in these views is more than semantic, because reverse microemulsions and clusters of nanodroplets retain high average curvature, while the average curvature in sponge phase bicontinuous microemulsions is low to vanishingly small. However, experimentally distinguishing these models has remained elusive.

Self-diffusion measurements by NMR of microemulsions have proven very useful in establishing transitions from oil-in-water to bicontinuous to water-in-oil isotropic phases [13]. This approach is particularly useful, because the diffusivity of each chemical component may be monitored more or less simultaneously. Sponge phase bicontinuity in microemulsions is inferred on the basis of the magnitude of self-diffusion coefficients [14,15]. In this paper we show that diffusion coefficients of intermediate magnitude arise natu-

rally in reverse microemulsions as a result of *partitioning* between continuous and discontinuous pseudophases. We further show that the detailed consideration of such partitioning provides means to quantify diffusivity arising from percolation, and to quantify the *volume* (fraction) of percolating cluster aggregates.

Electrochemical studies [16,17] have revealed a threshold phenomenon in Faradaic electron transfer involving electroactive species included in the aqueous phase of certain microemulsions. The redox chemistry appears to switch on when the cosurfactant chemical potential is raised above a certain critical threshold. This phenomenon was reminiscent of the percolation in electrical conductivity reported for a similar system [18], and was subsequently confirmed to coincide with the percolation threshold [19]. These Faradaic and conductivity thresholds are illustrated in Fig. 1 for reverse microemulsions of water in toluene, stabilized by the surfactant AOT (sodium bis[2-ethylhexyl]sulfosuccinate). Acrylamide is a cosurfactant [20] in this system, and its

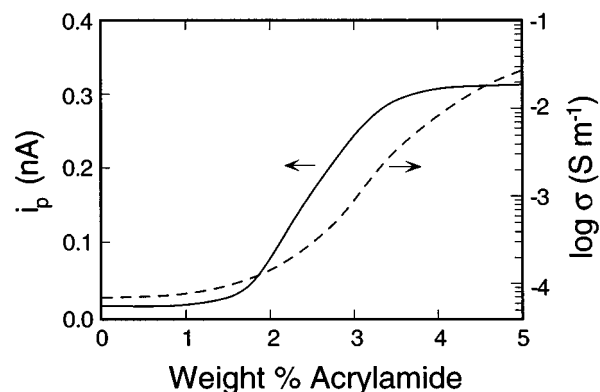


FIG. 1. Peak current (—) for oxidation of ferrocyanide and electrical conductivity (---) in water–acrylamide–AOT–toluene reverse microemulsions, as acrylamide composition is varied. Peak currents are from square wave voltammetry at 10- μ m-diam platinum microelectrodes. Microemulsions were formulated with 1.84 g AOT, 7.32 g toluene, 0.833 g aqueous 10 mM potassium ferrocyanide (—) or 0.833 g water (---), and varying amounts of acrylamide (0–0.65 g) to cover the range of 0–5% (w/w). Measurements were made at 25 °C.

chemical potential serves as a field variable in modifying the microstructure and increasing water solubilization, as well as inducing percolation.

The onset of percolation in this microemulsion system has been linked to physical changes within the interface, such as increased interfacial flexibility [18] and decreased chain packing order [19,21]. Such changes lead to increased interdroplet attraction, coalescence, and cluster formation. In this paper we further examine microstructure near the percolation threshold by considering the self-diffusion of all four components, water, AOT, toluene, and acrylamide. These data provide evidence for further distinguishing bicontinuity and clustering above percolation threshold.

Self-diffusion measurements for each of the four components in the microemulsions were determined by pulsed-gradient spin-echo (PGSE) NMR spectroscopy. This approach is based on the method of Stejskal and Tanner [22] and is derived from the nuclear spin echo concept of Hahn [23] and Carr and Purcell [24]. The diffusion coefficient is obtained from the attenuation of the spin echo under the influence of pulsed magnetic field gradients. Measurements were made at 25 ± 0.5 °C on a Varian Unity 500, narrow bore (51 mm) spectrometer operating at 499.9 MHz. The spectrometer was equipped with a commercially available diffusion system, which includes a 5 mm, ^1H - ^{19}F , air cooled, z -gradient probe built by Doty Scientific, a Highland DC current amplifier for producing current pulses, and a Sorrenson variable temperature power supply. The current amplifier was enhanced to provide up to 20 A; this enhancement allowed the probe to reach a gradient of up to 1000 G cm^{-1} with excellent stability.

We employed a stimulated-echo pulse sequence with long eddy current delay [25]. Eddy currents have been reduced and amplifier overdrive eliminated by using ramped (trapezoidal shaped) gradients [26]. Experiments were performed by varying the gradient strength (g) and keeping the gradient width (δ) and all other timing parameters constant. Typically, a value of 100 ms was used for the diffusion time (Δ). This value was chosen to insure that the mean displacement of the molecular center of mass was more than $10\,000 \text{ \AA}$ and thus much larger than any internal displacements relative to the center of mass. The relationship between the echo attenuation and self-diffusion coefficient is given by

$$\ln(E/E_0) = -D\gamma^2 g^2 \{ \delta^2 (\Delta - (\delta/3)) + (\epsilon^3/30) - \delta(\epsilon^2/6) \}, \quad (1)$$

where γ is the gyromagnetic ratio of the ^1H nucleus, E is the measured signal amplitude, E_0 is the amplitude with no gradients, and ϵ is the duration of the gradient ramp (200 μs). Half-echoes were acquired for typically 10 values of g and Fourier transformed. The natural logarithm of the integral value for the resonance of interest was recorded and plotted against g^2 . The value of D was obtained from the slope of a least-squares fit. The high magnetic field of the spectrometer resulted in excellent sensitivity and spectral dispersion.

Self-diffusion coefficients obtained from these data are displayed in Fig. 2 for each of the chemical components as a function of the acrylamide level. The water, acrylamide, and AOT data appear to exhibit breakpoints near the percolation threshold, in the neighborhood of 1.5–2 % acrylamide. It is

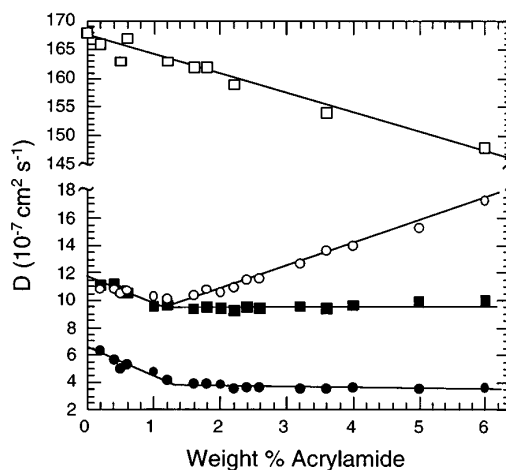


FIG. 2. Observed self-diffusion coefficients at 25 °C for toluene (\square), water (\circ), acrylamide (\blacksquare), and AOT (\bullet) in the microemulsions as a function of acrylamide content. The lines are included as guides to the eye.

noteworthy that the toluene self-diffusion is suppressed only 8% over the illustrated range in composition. This suppression is due to increasing viscosity and the particle obstruction. *Bulk* viscosity increases about three-fold over this composition range, from about 1.25 cP to about 4 cP. The water and acrylamide data initially coincide, below threshold, but diverge markedly above threshold. The AOT data run parallel to the acrylamide data, but are offset to lower values. Experiments were performed on the 4% (w/w) acrylamide sample to test for a diffusion time (Δ) dependence. Variations of 10–1000 ms in Δ did not yield any significant variation in the self-diffusion derived for each of the four chemical components.

We examine the AOT diffusion in the context of a fast exchange model, where it is assumed that the AOT exchanges between the water swollen droplets of the disperse pseudophase and the toluene-solvated unimeric state in the continuous (toluene) pseudophase. Therefore, the observed AOT diffusion may be modeled as a mole-fraction weighted average of the faster diffusing molecule in the continuous toluene phase (D_c) and the more slowly diffusing swollen micelle (D_{mic}) [27],

$$D_{\text{obs}} = xD_c + (1-x)D_{\text{mic}}. \quad (2)$$

The critical micelle concentration of AOT in toluene is of the order of that found in benzene [28], about 4×10^{-4} to $2 \times 10^{-3} \text{ M}$, with a geometric average of about $9 \times 10^{-4} \text{ M}$. We found the diffusion coefficient of AOT in the molecular state in toluene at 25 °C to be $1.29 \times 10^{-5} \text{ cm}^2 \text{ s}^{-1}$. The total volume concentration of AOT in the microemulsions is of the order of 0.4 M, so that the mole fraction (of AOT in the continuous pseudophase) $x \approx 0.002$. Essentially all of the AOT is in the disperse state, and we have, therefore, the quantitative estimate that $D_{\text{obs}} - D_{\text{mic}} \leq 3 \times 10^{-8} \text{ cm}^2 \text{ s}^{-1}$. Since D_{obs} for AOT ranges over $(3-6) \times 10^{-7} \text{ cm}^2 \text{ s}^{-1}$, we may take $D_{\text{mic}} \approx D_{\text{obs}}$ (D_{AOT}) with about 5–10 % error.

A local viscosity η was derived from the Stokes-Einstein equation and the assumption that the molecular size (diam-

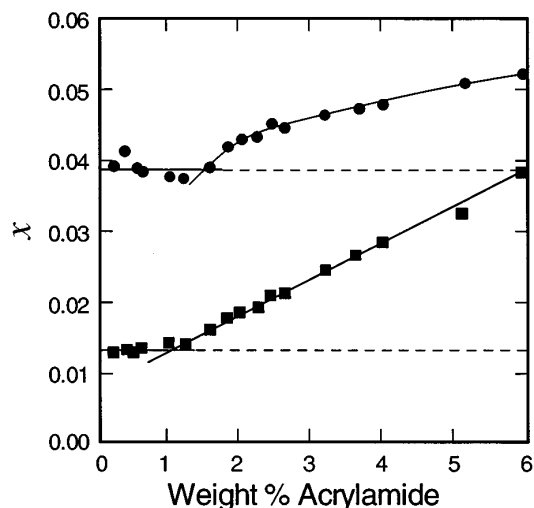


FIG. 3. Mole fraction (x) of acrylamide (●) and water (■) in the continuous (toluene) phase of the microemulsions as a function of acrylamide content. The lines are included as guides to the eye.

eter) of toluene is the same in neat toluene as it is in the microemulsions, the bulk viscosity of toluene, η^0 (0.558 cP), the self-diffusion of neat toluene, D_{tol}^0 ($2.26 \times 10^{-5} \text{ cm}^2 \text{ s}^{-1}$), at 25 °C, and the measured diffusion (D_{tol}) of toluene in the microemulsions:

$$\eta = \eta^0 (D_{\text{tol}}^0 / D_{\text{tol}}). \quad (3)$$

The diffusivity of acrylamide essentially parallels that of AOT, although it increases slowly as acrylamide concentration increases above the 1–2 % range. Acrylamide is also assumed to undergo rapid exchange between the continuous and disperse pseudophases, and the measured D_{obs} for acrylamide is also considered in terms of Eq. (2), where the resultant is a weighted average of the diffusivity in both pseudophases. The D_{mic} ($\approx D_{\text{AOT}}$) values obtained from the AOT diffusivity above are used. The D_c value was taken as the diffusivity of acrylamide we measured in toluene, $1.92 \times 10^{-5} \text{ cm}^2 \text{ s}^{-1}$ (D_{acryl}), adjusted for the local viscosity derived from the toluene viscosity, η^0/η :

$$D_c = (\eta^0/\eta) D_{\text{acryl}}^0. \quad (4)$$

The mole fraction of acrylamide in the respective pseudophases can then be calculated from Eq. (2), the observed diffusivity of acrylamide (Fig. 2), the observed diffusivity of AOT (D_{mic}), and the diffusivity of acrylamide in the continuous pseudophase, D_c [Eq. (4)]. Results are illustrated in Fig. 3. Also illustrated in Fig. 3 is the calculated [Eq. (2)] mole fraction of water in the continuous phase, where the viscosity corrected [Eq. (4)] diffusion of water at 25 °C in toluene ($5.41 \times 10^{-5} \text{ cm}^2 \text{ s}^{-1}$) was used for D_c .

Below 1.6% acrylamide, the mole fraction of acrylamide in the continuous phase appears relatively constant, at about $x=0.0387$. This value is depicted with a horizontal line that extends dashed to the right of the percolation threshold. The mole fraction of acrylamide in the continuous phase appears

to steadily increase above the threshold, but only increases about 38% above the equilibrium level obtained below threshold. A similar trend is observed for water, except that the amount of water apparently in the continuous phase increases by about 200% over the subthreshold value.

If partitioning of acrylamide and water between the particulate and continuous pseudophases were constant, we would expect all of the data in Fig. 3 to cluster about the respective horizontal lines. The apparent (differential) increases in partitioning into the continuous phase over the subthreshold values clearly suggest a quantification of these components in a new pseudophase, percolating aggregates and clusters. These differential increases indicate that a tripartite pseudophase model is appropriate, composed of the continuous and droplet pseudophases of the present analysis, and a percolating cluster pseudophase. In this model, we assume that the water to AOT molar ratio in the clusters is the same as that of the swollen micelles (≈ 11), and therefore the excess mole fraction derived for water in Fig. 3 approximately represents the *volume fraction* of the percolating pseudophase (φ_{clstr}). We may thereby derive an order parameter (S) for the disperse pseudophase,

$$S = \varphi_{\text{clstr}} / (\varphi_{\text{clstr}} + \varphi_{\text{mic}}), \quad (5)$$

where φ_{mic} is the volume fraction of the swollen micelle pseudophase. The results in Fig. 3 indicate S increases from 0 to about 0.027 as the acrylamide is added above the percolation threshold. We hypothesize that this order parameter would need to be of the order of 0.5 before a sponge phase bicontinuous microstructure could be reasonably inferred. A similar quantitative (partitioning) analysis of the apparent increase of acrylamide in the continuous phase (Fig. 3) shows that acrylamide *preferentially segregates* into the percolating clusters. This segregation underscores the role of the acrylamide chemical potential as a controlling field variable.

The order parameter obtained shows unequivocally that the onset of percolation corresponds to a second order or continuous-type transition. This transition occurs *within* a single phase isotropic thermodynamic domain, but corresponds to a pseudophase transition. Additionally, the order parameter provides means for quantifying the volume fraction of the percolating pseudophase. Such an order parameter should prove useful in quantitative evaluations of theories, once formulated, for the formation and growth of percolating clusters, and for the transformation [11] of such clusters to structures having low to zero mean curvature. In as much as the structure and dynamic nature of percolating clusters is not yet “well defined,” it is our expectation that further quantitative analyses and measures such as the order parameter introduced here will lead to improved understanding of such microstructure. An explicit three-state model will be discussed in detail subsequently. That model may be iterated to self-consistency, but these order parameter results are affected only very slightly, and no conclusions are qualitatively changed.

We gratefully acknowledge stimulating discussions on percolation-bicontinuity controversies with Björn Lindman, Ishi Talmon, and Max Almgren.

- [1] *Organized Solutions*, edited by S. E. Friberg and B. Lindman (Marcel Dekker, New York, 1992).
- [2] M. Borkovec, H.-F. Eicke, H. Hammerich, and B. Das Gupta, *J. Phys. Chem.* **92**, 206 (1988).
- [3] S. A. Safran, in *Micellar Solutions and Microemulsions-Structure, Dynamics and Statistical Thermodynamics*, edited by S.-H. Chen and R. Rajagopalan (Springer-Verlag, New York, 1990), pp. 161–184.
- [4] M. W. Kim and W. D. Dozier, in *Micellar Solutions and Microemulsions-Structure, Dynamics and Statistical Thermodynamics* (Ref. [3]), pp. 291–301.
- [5] L. E. Scriven, *Nature (London)* **263**, 123 (1976).
- [6] B. Lagourette, J. Peyrelasse, C. Boned, and M. Clause, *Nature (London)* **281**, 60 (1979).
- [7] D. Chatenay, W. Urbach, A. M. Cazabat, and D. Langevin, *Phys. Rev. Lett.* **54**, 2253 (1985).
- [8] M. Lagües, *J. Phys. (France) Lett.* **40**, L331 (1979).
- [9] R. Johannsson and M. Almgren, *Langmuir* **9**, 2879 (1993).
- [10] S.-H. Chen, S.-L. Chang, and R. Strey, *J. Chem. Phys.* **93**, 1907 (1990).
- [11] A.-M. Cazabat, D. Chatenay, D. Langevin, and J. Meunier, *Faraday Discuss. Chem. Soc.* **76**, 291 (1982).
- [12] R. T. Hamilton, J. F. Billman, and E. W. Kaler, *Langmuir* **6**, 1696 (1990).
- [13] M. T. Clarkson, D. Beaglehole, and P. T. Callaghan, *Phys. Rev. Lett.* **54**, 1722 (1985).
- [14] B. Lindman, N. Kamenka, T.-M. Kathopoulos, B. Brun, and P.-G. Nilsson, *J. Phys. Chem.* **84**, 2485 (1980).
- [15] P. Guéring and B. Lindman, *Langmuir* **1**, 464 (1985).
- [16] E. García and J. Texter, *Proc. Electrochem. Soc.* **93-1**, 2166 (1993).
- [17] E. García, S. Song, E. Oppenheimer, B. Antalek, A. J. Williams, and J. Texter, *Langmuir* **9**, 2782 (1993).
- [18] M. T. Carver, E. Hirsch, J. C. Whittmann, R. M. Fitch, and F. Candau, *J. Phys. Chem.* **93**, 4867 (1989).
- [19] B. Antalek, A. Williams, E. García, D. H. Wall, S. Song, and J. Texter, in *Dynamic Properties of Interfaces and Association Structures*, edited by V. Pillai and D. O. Shah (AOCS Press, Champaign, IL, 1996), pp. 183–196.
- [20] H. F. Eicke, *J. Colloid Interface Sci.* **68**, 440 (1979).
- [21] B. Antalek, A. J. Williams, E. García, and J. Texter, *Langmuir* **10**, 4459 (1994).
- [22] E. O. Stejskal and J. E. Tanner, *J. Chem. Phys.* **42**, 288 (1965).
- [23] E. L. Hahn, *Phys. Rev.* **80**, 580 (1950).
- [24] H. Y. Carr and E. M. Purcell, *Phys. Rev.* **94**, 630 (1954).
- [25] S. J. Gibbs and C. S. Johnson, *J. Magn. Reson.* **93**, 395 (1991).
- [26] W. S. Price and P. W. Kuchel, *J. Magn. Reson.* **94**, 133 (1991).
- [27] P. Stilbs and B. Lindman, *Prog. Colloid. Polym. Sci.* **69**, 39 (1984).
- [28] M. Ueno and H. Kishimoto, *Bull. Chem. Soc. Jpn.* **50**, 1631 (1977).